A TWO-PHASE OPTIMIZATION METHOD FOR THE EXPANSION PLANNING OF DISTRICT HEATING SYSTEMS USING DIFFERENT DISCRETIZATION TECHNIQUES

Jerry Lambert[1]*, Hartmut Spliethoff[1]

[1]Technical University of Munich, Chair of Energy Systems, Munich, Germany

*Corresponding Author: jerry.lambert@tum.de

ABSTRACT

The current high costs of district heating systems set limits regarding the minimum heat demand density required for economic network expansions. Optimized routing with ideal pipe sizing offers a potential for cost reduction. Therefore, this paper introduces a two-phase method for district heating network expansion planning. This method consists of consecutive optimizations, starting with a mixed-integer linear programming followed by a nonlinear optimization. During the mixed-integer linear programming, the district heating system is optimized with continuous diameters, and the nonlinear pressure and temperature dependencies must be linearized. The resulting topology and the continuous diameters are afterward handed over to a nonlinear sparse sequential quadratic programming. During this second phase, the continuous diameters have to be discretized. This study investigates a rational approximation of material properties and a tangent hyperbolic penalization method. Different versions of these methods with varying diameter ranges (two and three available diameters) and penalization directions are studied. The results of this study indicate that methods without changing penalization methods within the same optimization problem provide higher accuracy in the discretization of the pipe's diameter. Moreover, if the accuracy of the discretized diameter should be emphasized during the optimization, penalization methods considering only two diameters should be preferred over penalization methods considering three diameters. Vice-versa, if obtaining the lowest possible diameters is prioritized over the accuracy of the discretization, methods considering three diameters should be preferred.

1 INTRODUCTION

In 2020, 85 % of the CO_2-emissions in German households resulted from space heating and hot water usage (Umweltbundesamt, 2023). Moreover, on a European level, 50 % of the final energy demand in 2015 was used for the heating and cooling sector (Fleiter et al., 2017). District heating can play a significant role in replacing the mostly fossil-based provision of heat with renewable energy sources due to numerous advantages over a building-specific heat supply (Werner, 2017). Those include the utilization of additional renewable energy sources, such as deep geothermal energy, the integration of seasonal energy storages, the possibility of waste heat recycling, higher heat generation efficiencies, and simultaneity factors occurring within the network while planning for production capacities (Jodeiri et al., 2022). To overcome the high initial investment costs of district heating systems (Nussbaumer and Thalmann, 2016), an optimized topology with ideal pipe sizing could offer one possibility to aid decision-makers in finding well-suited areas for district heating systems and aid to speed up the heating sector's transformation. The following paragraphs briefly overview different optimization techniques used for district heating systems. Those include mixed-integer linear programming (MILP), mixed-integer nonlinear programming (MINLP), heuristics, and nonlinear programming (NLP) using the adjoint method.

Sporleder et al. (2022) evaluated 51 publications and found that around 80 % use MILP or linear models to optimize district heating systems. This arises from the discrete nature of the optimization problem,

https://doi.org/10.52202/077185-0022

as shown in (Söderman, 2007), where the pipe's concave investment cost function is approximated by a fixed and a size-dependent part. Söderman and Pettersson (2006) implement a MILP to optimize a distributed energy system, including district heating and storage. Dorfner and Hamacher (2014) use a similar approach to optimize the topology of a single-commodity flow network. Dorfner et al. (2017) expand their work to consider district cooling systems and to incorporate redundancy constraints against the unavailability of each considered cooling station. In both studies, the optimization is reduced to a network power flow, neglecting, e.g., mixing effects at junctions and pressure dependencies. Résimont et al. (2021) improve the problem formulation of Dorfner et al. (2017) by removing redundant definitions of decision variables. Moreover, based on Dorfner et al. (2017), Röder et al. (2021) introduce a new model with fewer binary variables. In the second step of the optimization procedure, pressure losses are estimated in the network at the heat demand's peak load, and the pipe diameters are sized accordingly. However, none of these methods can depict the nonlinear effects of district heating networks. Flow patterns in systems with multiple spatial distributed producers, mixing temperatures at junctions or loops, can hardly be linearized while respecting the physical interrelations.

Deng et al. (2017) propose a MINLP to consider the nonlinearities within the district heating network and to solve an operational-based optimal scheduling strategy to minimize the daily operational cost of an energy station with a heating and cooling demand and storage. However, the heat distribution by a district heating network is neglected, and the network's topology is not optimized. A nonlinear discrete representation of a steady-state district heating system is solved by (Mertz et al., 2016). Mertz et al. (2017) apply the same method to a small network with 19 consumers. In contrast to MILP, MINLP is often limited to smaller districts due to the nonlinear equations in combination with integer variables. Wack et al. (2023b) can show that solving the full MINLP leads to exponentially scaling computational costs with increasing network size during the discrete topology optimization.

In large combinatorial problems, where finding an optimal solution is difficult, heuristics can be an approach to finding an approximate solution. Heuristic approaches commonly use nature-inspired algorithms like the ant colony optimization or the genetic algorithm. Allen et al. (2022) investigate a particle swarm optimization to find the best subset of buildings that should be connected to the district heating network. Moreover, a minimum spanning tree heuristic was applied to find a network topology (Allen et al., 2022). Merlet et al. (2022) find the optimal sizing of pipe diameters using a genetic algorithm to generate a set of Pareto-optimal sizing choices. On the downside, heuristics may provide a sufficiently good solution to an optimization problem while not always guaranteeing a local or global optimum. This becomes especially difficult with scaling dimensions of the optimization problem.

Wack et al. (2023a) propose a nonlinear optimization method where intermediate diameters are penalized, and the optimization problem is solved with an adjoint optimization method. The adjoint method is a numerical method for efficiently computing a function's gradient during an optimization problem. Pizzolato et al. (2018) use the adjoint method to optimize robust hydraulic district heating systems while neglecting thermal aspects within the network.

Based on the penalization method of Wack et al. (2023a) and the previous work of Lambert and Spliethoff (2023) and Lambert et al. (2024), this paper investigates different penalization methods to discretize continuous diameters from a MILP in a subsequent NLP. Moreover, the penalization's benefit is investigated and compared to a simple rounding up to the next larger discrete diameter. Therefore, a rational approximation of material properties approach and a solid isotropic material-like penalization approach are applied to the nonlinear district heating model.

2 A TWO-PHASE NONLINEAR THERMO-HYDRAULIC TRANSPORT MODEL

Lambert and Spliethoff (2023) introduce a hybrid optimization strategy consisting of two optimization phases and a single optimization time step (the maximal peak load case) to determine a district heating system's routing and pipe sizing. A detailed description of both optimization phases is shown in Lambert and Spliethoff (2023). The district is optimized in the first phase with a MILP and continuous diameters.

https://doi.org/10.52202/077185-0022

Based on the continuous diameter determined by the MILP, the choice of the available diameter in the subsequent sequential quadratic programming (SQP) is limited. Moreover, the flow direction is set according to the direction optimized by the MILP. The continuous diameters are discretized during the second phase of the optimization, and a nonlinear thermo-hydraulic flow model is calculated. In this paper, the considered heat carrier medium is water. It is assumed to be liquid and, therefore, incompressible. Additionally, by assuming temperature changes smaller than $\Delta T = 40$ °C, temperature dependencies of the fluid properties (e.g., density ρ, heat capacity c_p and dynamic viscosity μ) are neglected, because the variations in the property values are small for the considered parameter range. The fluid properties of water are constant and determined at 70 °C. In order to calculate the pressure loss between two nodes i and j with an inner pipe diameter d_{ij} of length l_{ij}, the pressure loss Δp_{ij} is calculated with the fluid's velocity v_{ij} according to Darcy-Weißbach:

$$\Delta p_{ij} = f_{ij} \cdot \frac{l_{ij}}{d_{ij}} \cdot \frac{v_{ij}^2}{2} \cdot \rho \tag{1}$$

The friction factor f_{ij} with the Reynold's number Re_{ij} is given by the Moody equation with the pipe roughness k: (Moody, 1947)

$$f_{ij} = 0.0055 \cdot \left[1 + \left(2 \cdot 10^4 \cdot \frac{k}{d_{ij}} + \frac{10^6}{Re_{ij}}\right)^{\frac{1}{3}}\right] \tag{2}$$

Next, the temperature loss through an insulated pipe buried underground is considered. Therefore, the temperature difference Θ between the water temperature in the pipe T and the outside temperature T_∞ is introduced. Here, T_∞ is set to -20 °C. This can be seen as a worst-case scenario, where the district heating network still must be able to supply the required heat to each customer. The exit temperature $\Theta_{ij} = T_{ij} - T_\infty$ of a pipe segment ij due to heat loss to its environment with an entry temperature Θ_i is given by:

$$\Theta_{ij} = \Theta_i \cdot \exp\left(\frac{-l_{ij}}{c_p \cdot \dot{m}_{ij} \cdot R_{ij}}\right) \tag{3}$$

In equation (3), the combined thermal resistance of the pipe and the soil per unit length is calculated with the ratio r between the pipe's outer and inner diameter, the heat conductivity of the ground λ_g and the insulation material of the pipe λ_{insul}, and the depth h of the buried pipe: (Blommaert et al., 2020)

$$R_{ij} = \frac{\ln\left((4h)/(rd_{ij})\right)}{2\pi\lambda_g} + \frac{\ln(r)}{2\pi\lambda_{insul}} \tag{4}$$

2.1 First Phase: Mixed Integer Linear Programming Optimization

Equation (1) is used to calculate a maximal thermal power flow for each considered piping diameter under consideration of a maximal length-specific pressure drop. Subsequently, this power flow is used to linearize the investment cost and the pipes' heat losses (using equation (3)). The thermal power in- and output ($\dot{Q}_{ij,0}$ *and* $\dot{Q}_{ij,1}$) of each pipe are modeled according to the network's directed graph. In order to allow flows in the opposite direction, every potential pipe ij is also modeled in the direction ji. In the following, only the equations in direction ij are discussed below. The heat balance of each pipe connecting node i and j is given by:

$$\dot{Q}_{ij,0} - \dot{Q}_{ij,1} - \left(a_{therm} \cdot \dot{Q}_{ij,0} + b_{therm} \cdot \lambda_{ij}\right) \cdot l_{ij} = 0 \tag{5}$$

The thermal losses in equation (5) are determined by the linear regression coefficients a_{therm} and b_{therm}. The binary variable λ_{ij} represents the flow direction of each pipe. Moreover, to enforce zero thermal power flow if the direction ij is not used, the following constraint with a sufficiently large constant power $\dot{Q}_{max,cons}$ is modeled $\dot{Q}_{ij,0} \leq \dot{Q}_{max,cons} \cdot \lambda_{ij}$. Each consumer connection to the district heating grid is modeled as unidirectional. Moreover, energy conservation is assumed in every node n under consideration of the consumer's heat demand ($\dot{Q}_{n,c}$) and the heat source's feed-in ($\dot{Q}_{p,n}$):

$$\dot{Q}_{ni,0} - \dot{Q}_{jn,1} - \dot{Q}_{n,c} + \dot{Q}_{p,n} = 0 \tag{6}$$

https://doi.org/10.52202/077185-0022

To ensure a unidirectional use of a pipe, an additional constraint preventing the simultaneous use of the direction ij and ji is used ($\lambda_{ij} + \lambda_{ji} \leq 1$). The thermal power output $\dot{Q}_{p,n}$ of each producer is constrained by the installed thermal capacity of the source $\dot{Q}_{p,inst}$, where $\dot{Q}_{p,n} \leq \dot{Q}_{p,inst}$. The annuity method distributes investment costs of pipes or heat sources over the defined life span n_{years}. Without discounting, the annuity an is calculated with an interest rate w as:

$$an = \frac{(1+w)^{n_{years}} \cdot w}{(1+w)^{n_{years}} - 1} \tag{7}$$

Finally, the objective function minimizes the district heating network's total investment and operational costs. The investment costs are determined by the linear regression factors a_{inv} and b_{inv}. By introducing full load hours flh for the heat demands of consumers, the investment and fuel costs ($c_{inv,p}$ and $c_{fuel,p}$) are weighted:

$$\min \left\{ \sum_p \dot{Q}_{p,inst} \cdot c_{inv,p} \cdot an_p + \sum_p \dot{Q}_p \cdot c_{fuel,p} \cdot flh + \sum_{ij} \left(a_{cost} \cdot \left(\dot{Q}_{ij,0} + \dot{Q}_{ji,0} \right) + b_{cost} \cdot \left(\lambda_{ij} + \lambda_{ji} \right) \right) \cdot l_{ij} \cdot an_{pipe} \right\} \tag{8}$$

The initially assumed flow direction in the graph can be corrected according to λ_{ij} and λ_{ji}: The pipe is not used and can be deleted from the graph ($\lambda_{ij} = 0$ and $\lambda_{ji} = 0$). The assumed flow direction in the graph is correct ($\lambda_{ij} = 1$ and $\lambda_{ji} = 0$) or the flow direction in the graph is the opposite of the assumed one and needs to be corrected ($\lambda_{ij} = 0$ and $\lambda_{ji} = 1$).

2.2 Second Phase: Nonlinear Programming Optimization

To account for more complex dependencies, such as pressure or temperature drops, a nonlinear optimization model has to be developed. By combining equations (1) and (2), the pressure loss between nodes i and j connected by a pipe with the mass flow $\dot{m}_{ij} = \rho \cdot v_{ij} \cdot d_{ij}^2 \cdot \pi/4$ can be calculated as:

$$p_i - p_j = \frac{8 \cdot f_{ij}}{\pi^2 \cdot \rho} \cdot \frac{l_{ij}}{d_{ij}^5} \cdot \dot{m}_{ij}^2 \tag{9}$$

Analogical to the thermal power flow calculation, a maximal length specific pressure $p_i - p_j \leq \Delta p_{ij,max} \cdot l_{ij}$ is imposed. Moreover, in each node, mass conservation must be fulfilled. Inside each node of the district heating system, perfect mixing of the incoming fluids is assumed. Therefore, all outgoing flows depart from the node with the corresponding node temperature, and energy is conserved. The heat losses in a pipe are determined by equation (3). However, a fixed ratio r between the outer and inner diameter of a pipe is assumed. Here, r is set according to the upper and lower allowed inner diameter, where r is the mean of the ratio of both thresholds. Overall, during the nonlinear optimization, the following equation is minimized, comprised of the pumping, the fuel, and the pipe's investment costs:

$$\min \left\{ \frac{\dot{m}_p \cdot \Delta p_p \cdot flh \cdot c_{el,pump}}{\rho \cdot \eta_{pump}} + \dot{m}_p \cdot c_p \cdot \Delta \Theta_p \cdot flh \cdot c_{fuel} + C_{inv,pipes} \right\} \tag{10}$$

The investment costs $C_{inv,pipes}$ are linearly interpolated between the upper and lower diameter's investment costs ($c_{inv,min}$ and $c_{inv,max}$):

$$C_{inv,pipes} = c_{inv,min} + \left(c_{inv,max} - c_{inv,min} \right) \cdot \frac{d - d_{min}}{d_{max} - d_{min}} \tag{11}$$

3 DISCRETIZATION METHODS FOR LINEAR PIPING DIAMETERS

This section presents different methods to discretize the continuous pipe diameters obtained by the MILP during the nonlinear optimization. In structural optimization, it can be desirable to substitute the

https://doi.org/10.52202/077185-0022

discrete variables with continuous variables and identify a means to iteratively force the solution towards a discrete solution (Deaton and Grandhi, 2014). Therefore, intermediate diameters have to be penalized. The first introduced penalization is the rational approximation of material properties, and the second is a solid isotropic material-like penalization approach using a tangent hyperbolic.

3.1 Rounding Continuous diameters

The simplest discretization method is rounding the continuous diameters up to the next upper commercially available diameter (d_{dis}). This method does not rely on the second phase of the optimization. It is used in this study as a base case to compare the effectiveness of the nonlinear modeling and the different discretization methods. Alternatively, rounding to the nearest DN (and choosing potentially smaller diameters as the continuous diameter) could lead to invalid diameter choices, which do not respect all imposed constraints (e.g., the maximal length specific pressure drop). This method is usually performed after MILP optimization to get discrete diameters, for example, in Röder et al. (2021).

3.2 Rational Approximation of Material Properties

Sigmund (2001) introduces the rational approximation of material properties method (RAMP) as an alternative to the solid isotropic material with penalization method (SIMP) (Deaton and Grandhi, 2014). Unlike SIMP, the RAMP method has a nonzero sensitivity when the variable is forced towards 0. Therefore, the RAMP model has been shown to alleviate some numerical problems at void conditions (Deaton and Grandhi, 2014). For a variable $x \in [0, 1]$ the RAMP penalization P is calculated with the penalization factor q as followed: (Sigmund, 2001)

$$P_{ramp}(x, q) = \frac{x}{1 + q \cdot (1 - x)} \tag{12}$$

Depending on the value q in equation (12), the direction of the penalization can be controlled (sub or above linear). Based on the continuous diameter determined by the MILP, the choice of the available diameter in the subsequent SQP is limited to the nearest commercially available diameter (d_{min}) and the next larger one (d_{max}). In order to use the RAMP projection, the continuous diameter variable d in equations (3) and (9) are substituted with the projected diameter $\bar{d}$:

$$\bar{d} = d_{min} + (d_{max} - d_{min}) \cdot P_{ramp}\left(\frac{d - d_{min}}{d_{max} - d_{min}}, q\right) \tag{13}$$

The importance of the penalization's direction should be shown for the pressure loss calculation (equation (9)). As for a choice of $q = 6$, the penalization of $\bar{d}$ leads to an increased pressure loss for non-discrete diameters while $q = -0.87$ to a decreased pressure loss. In Figure 1(a), the projected diameter using equation (12) is shown, and Figure 1(b) depicts the influence of the penalization direction on the pressure loss equation. All investigated penalization methods using the RAMP method are summarized in Table 1.

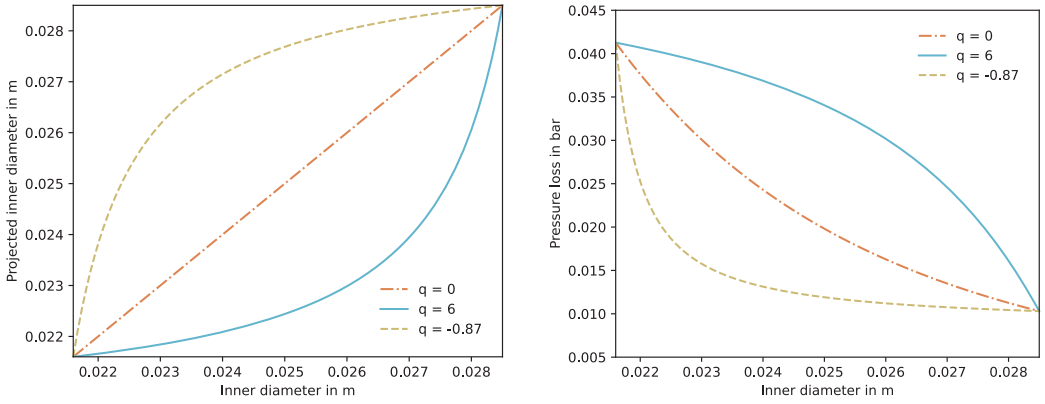

(a) Projected diameter using RAMP. **(b)** Pressure loss calculation using RAMP.

Figure 1: Penalization of intermediate piping diameters using RAMP.

https://doi.org/10.52202/077185-0022

Table 1: Investigated penalization methods using the RAMP method

Name	Choice of diameters	q for $\bar{d}$ in equation (9)	q for $\bar{d}$ in equation (4)
Ramp_1	2	{0, -0.67, -0.87}	{0, -0.67, -0.87}
Ramp_2	2	{0, 2, 6}	{0, -0.67, -0.87}

Moreover, $C_{inv,pipes}$ in equation (10) is substituted by the following penalized investement calculation:

$$C_{inv,pipes}(d) = c_{inv,min} + \left(c_{inv,max} - c_{inv,min}\right) \cdot P_{ramp}\left(\frac{d - d_{min}}{d_{max} - d_{min}}, q\right) \tag{14}$$

3.3 A Solid Isotropic Material-like Penalization Approach using a Tangent Hyperbolic

Another method to penalize intermediate diameters is the use of tangent hyperbolics, approximating a smooth heavyside function. This method is adapted from Wack et al. (2023a). Here a variable $x \in [0, 1]$ is projected onto the discrete set of $\{0, 1\}$ by using:

$$P_{\tanh}(x, q, a) = \frac{\tanh\left(q \cdot (x - a)\right)}{\tanh(q)} + a \tag{15}$$

In equation (15), the steepness of the projection is controlled by q, while the direction is controlled by $a \in \{0, 1\}$. Similar to equation (13), the choice of the available diameter in the subsequent SQP is limited to the nearest commercially available diameter and the following larger one:

$$\bar{d} = d_{min} + (d_{max} - d_{min}) \cdot P_{tanh}\left(\frac{d - d_{min}}{d_{max} - d_{min}}, q, a\right) \tag{16}$$

Moreover, the possibility of providing more than two discrete diameters to the subsequent NLP should be investigated. Therefore, based on Wack et al. (2023a), equation (16) is expanded to consider three discrete diameters. The three available diameters are: the nearest discrete diameter (d_{mid}), the next upper discrete diameter (d_{max}), and the next lower discrete diameter (d_{min}):

$$\begin{aligned}\bar{d} = d_{min} &+ (d_{mid} - d_{min}) \cdot \min\left(P_{tanh}\left(\frac{d - d_{min}}{d_{mid} - d_{min}}, q, a\right), 1\right) \\ &+ (d_{max} - d_{mid}) \cdot \max\left(P_{tanh}\left(\frac{d - d_{mid}}{d_{max} - d_{mid}}, q, a\right), 0\right)\end{aligned} \tag{17}$$

The minimum and maximum functions in equation (17) must be smoothly approximated. Therefore, a Boltzmann operator is used:

$$S_\alpha(x_1, \cdots, x_n) = \frac{\sum_{i=1}^{n} \mathrm{x_i} \cdot \exp(\alpha \cdot x_i)}{\sum_{i=1}^{n} \exp(\alpha \cdot x_i)} \tag{18}$$

In equation (18), if $\alpha \to +\infty$, S_α approximates a maximum of $x_1, \cdots, x_n$. If $\alpha \to -\infty$, S_α approximates a minimum of $x_1, \cdots, x_n$. Finally, the maximum and minimum function can be approximated with:

$$\max(x, 0) = \frac{x}{1 + \exp(-\alpha \cdot \mathrm{x})} \tag{19}$$

$$\min(x, 1) = \frac{1 + x \cdot \exp\left(-\alpha \cdot (\mathrm{x} - 1)\right)}{1 + \exp\left(-\alpha \cdot (\mathrm{x} - 1)\right)} \tag{20}$$

All investigated penalization methods using a tangent hyperbolic are summarized in Table 2. The penalized investment costs are determined analogical to section 3.2.

Table 2: Investigated penalization methods using tangent hyperbolic

Name	Choice of diameters	a in equation (9)	a in equation (4)
TH_1	2	0	0
TH_2	2	1	0
TH_3	3	0	0
TH_4	3	1	0

https://doi.org/10.52202/077185-0022

4 APPLICATION TO FOUR REAL-WORLD DISTRICTS

This section presents the resulting inner diameters for four different real-world districts with an increasing number of consumers. The data for each district is taken from Lambert and Spliethoff (2024). All calculations are performed on an Intel© dual Xeon© E5-2699 v3 CPU with 2.3 GHz, 18 physical cores, and 256 GB of RAM. During the first phase, the optimization is solved with Gurobi© 10.0.2 (Gurobi Optimization, 2023) and a required minimum relative MIP-Gap of 0.1 %. The standard seed and settings of Gurobi© 10.0.2 are used during the optimization, and the problem formulation is done in Pyomo (Hart et al., 2011). The second phase is formulated with pyoptsparse (Wu et al., 2020) and solved with the SQP solver SNOPT 7.7.7 (Stanford Business Software Inc, 2021). The optimization is performed with boundary conditions, shown in Table 3. The investment costs for piping diameters (ranging from DN 20 to DN 400) are adapted from Nussbaumer and Thalmann (2016).

Table 3: Boundary parameters considered in the optimization

Parameter	Value	Reference
Full Load hours (referenced to kW_{peak})	2500 h	(European Commission, 2018)
Heat production costs	0.08 €/kWh	(AGFW, 2024)
Service life of pipes	40 a	o.a.
Interest rate for district heating pipes	8 %	(AGFW, 2024)
Electricity Costs	0.2 €/kWh	o.a.
Pumping Efficiency	70 %	o.a.
Feed temperature at the producer	90 °C	o.a.
Return temperature at each consumer	55 °C	o.a.
Penalization factor RAMP	{0, 2, 6}, {0, -0.67, -0.86}	(Krogh et al., 2017)
Penalization factor Heaviside function	{0, 1.5, 4}	o.a.
Factor α for smooth max and min	3	o.a.

o.a. is an abbreviation for own assumption

Table 4 shows the number of potential pipes and consumers in the four districts. Each consumer has to be connected to the district heating grid, regardless of the profitability of the individual connection. The number of pipes is shown for the initial district and the optimized district after the first phase. During the first phase, the topology of each district is optimized, and an initial guess for pipe sizing is provided for the nonlinear optimization. The full nonlinear thermo-hydraulic model is solved iteratively during the second phase with increasing penalization factors, shown in Table 3. In order to initialize the nonlinear optimization, the penalization factor 0 indicates the use of the continuous diameter variables and the use of the non-penalized equations (3) and (9).

Table 4: Number of pipes and consumers in each considered district after the first optimization phase

District	Number of Pipes (Initial)	Number of Pipes (After Phase 1)	Number of Consumers
District 1	788	725	400
District 2	1038	985	567
District 3	1695	1499	794
District 4	1972	1798	959

In Figure 2, the orange point represents the heat source, gray nodes junctions, and blue nodes consumer within the district heating system. Figure 2(a) shows the initial district heating system given to the MILP. The district consists of 1038 edges, reduced to 726 edges during the first phase, and 400 consumers with a total heat demand of 4403.57 kW_{peak}. Figure 2(b) shows the resulting final district heating system with the discretized diameters. Here, the thickness of a pipe corresponds to the size of a pipe.

https://doi.org/10.52202/077185-0022

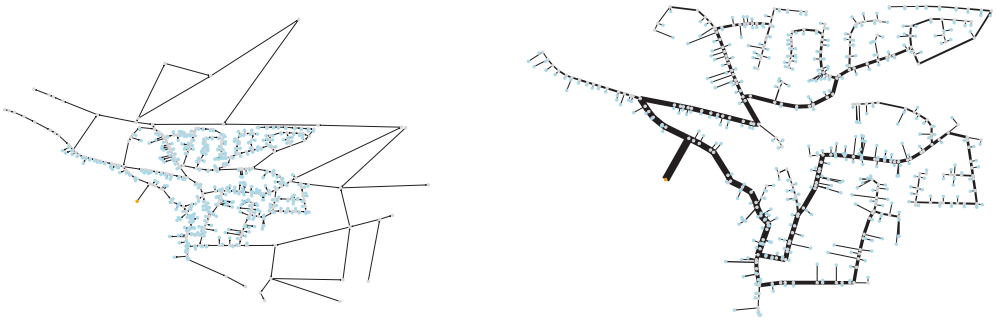

(a) Initial district heating **(b)** Optimized district heating system

Figure 2: Initial and optimized district heating system (District 1, TH_1).

Figure 3 shows the resulting nonlinear pressure and temperature profiles of District 1 after the second phase. The highest cumulative pressure losses can be observed at the most remote consumer, defining the pressure level at the heat source. As every consumer has to be connected to the grid, a considerable temperature drop can be observed in some pipes. This is due to those consumers' very low heat demand and the choice of available diameters. The smallest possible pipe is DN 20 (corresponding to an inner diameter of 0.0216 m), which is often oversized for those small heat loads.

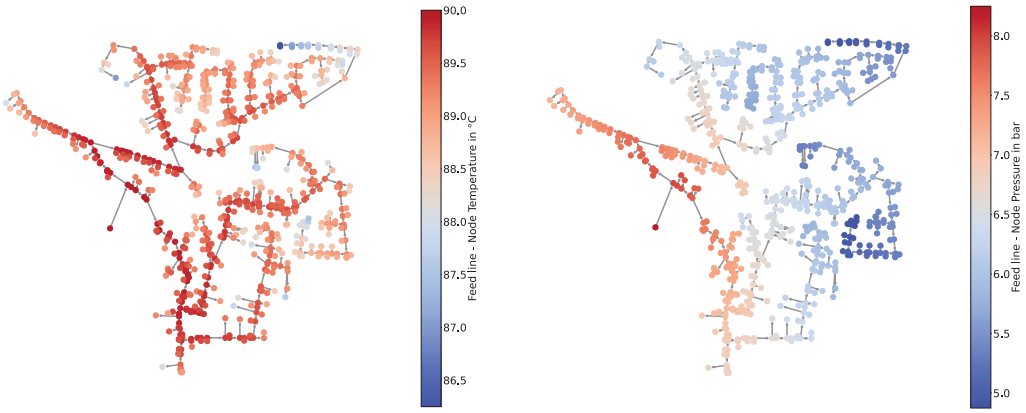

(a) Temperature profile. **(b)** Pressure profile.

Figure 3: Resulting nonlinear temperature and pressure profile (feed line, district 1).

4.1 Deviation from Discrete Diameters

In this section, the deviation from discrete diameters is presented. To determine the deviation from the nearest commercially available pipe diameters d_{dis}, the mean absolute percentage error $MAPE$ is used:

$$MAPE = 100 \cdot \frac{1}{n_{pipes}} \cdot \sum_{i=1}^{n_{pipes}} \frac{abs(d_i - d_{dis})}{d_{dis}} \tag{21}$$

Moreover, the mean deviation MD is used to characterize the error made during the penalization:

$$MD = \frac{1}{n_{pipes}} \cdot \sum_{i=1}^{n_{pipes}} \frac{d_i}{d_{dis}} \tag{22}$$

Table 5 shows each penalization method and district's $MAPE$ and MD. Here, the methods that only consider two diameters outperform, in most cases, the methods that consider three different diameters.

https://doi.org/10.52202/077185-0022

Moreover, the methods with changing penalization directions, for example, Ramp_2 or TH_2, cannot discretize the diameters as well as the counterparts without changing penalization directions. Ramp_2, TH_2, and TH_4 are also more likely to slightly discretize the pipe diameter below the discrete value, while Ramp_1, TH_1, and TH_3 tend to discretize the piping diameter above the discrete value.

Table 5: Mean absolute error and relative deviation for each district and penalization method

District	Ramp_1		Ramp_2		TH_1		TH_2		TH_3		TH_4	
	MAPE	MD	MAPE	MD	MAPE	MD	MAPE	MD	MAPE	MD	MAPE	MD
1	0.39	1.01	1.56	0.99	0.60	1.01	1.84	0.99	1.55	1.01	2.62	1.00
2	0.41	1.01	2.14	0.99	0.65	1.01	4.24	0.99	2.08	1.01	3.07	0.99
3	0.34	1.01	1.74	1.01	0.53	1.01	1.56	0.99	2.55	1.02	1.68	0.98
4	0.43	1.01	1.92	0.99	0.77	1.01	2.24	0.99	2.08	1.01	2.03	0.98

Figure 4 shows the considered penalization method's absolute percentage error for each pipe in all of the four districts. Overall, TH_3 and TH_4 discretize the piping diameter with the most significant absolute percentage error distribution, while Ramp_1 and TH_1 achieve the smallest one. The median of the absolute percentage error for the studied penalization methods is near zero. Therefore, continuous diameters close to an upper or lower bound are often discretized pretty accurately. This is often the case for pipes connecting consumers to the main district heating grid. For penalization methods, considering three different diameters, especially the intermediate diameters d_{mid} exhibit the highest discretization errors, and, thus, TH_3 and TH_4 have the largest error distribution.

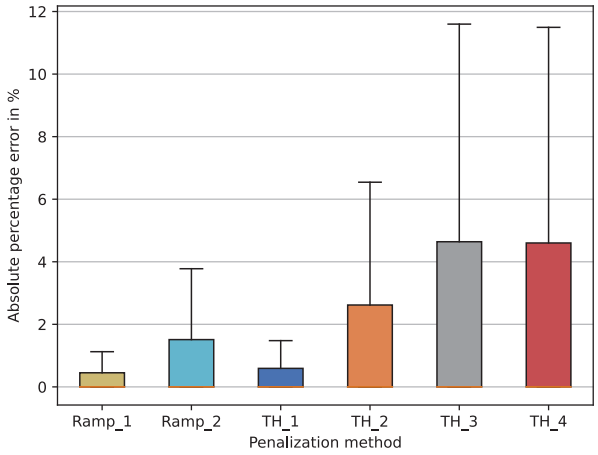

Figure 4: Absolute percentage error for each pipe in the four districts for each penalization method.

If the accuracy of the discretized diameter should be emphasized during the optimization, penalization methods considering two diameters should be preferred over penalization methods considering three diameters. Moreover, changing penalization directions in different equations within the same optimization problem leads to a lower discretization accuracy.

4.2 Investment Costs and Mean Diameter

In order to compare the effectiveness of the discretization methods, each penalization method should be compared to a simple rounding up to the next diameter. Therefore, the mean diameter d_{mean} of the pipes in the district heating system is used, calculated with the total length l_{tot} of the district heating system:

$$d_{mean} = \sum_{i=1}^{N_{pipe}} \frac{l_i \cdot d_i}{l_{tot}} \tag{23}$$

https://doi.org/10.52202/077185-0022

If a discretization method did not converge to a fully discrete value, the nearest discrete diameter is used in equation (23). Table 6 shows the mean diameter for each district and penalization method compared to rounding the continuous diameters up to the next upper commercially available diameter. Each considered penalization method can find a lower mean diameter than the rounding method (excpet for TH_2 in district 2). However, the penalization methods considering three diameters (TH_3 and TH_4) achieve the lowest mean diameter. On the one hand, this is due to the larger selection of diameters from which the optimizer can choose. As the choice of the available diameter is limited to the following commercially available diameter and the following larger one for Ramp_1 and TH_1, it can sometimes be beneficial to consider one additional smaller diameter. The heat losses are overestimated for small diameters in the linearization during the optimization's first phase. This trend is reversed starting at DN 65. Therefore, depending on the initial diameter and the pipe position within the network, the pipe diameter can sometimes be best adjusted with three possible diameters. On the other hand, by considering only two diameters, the optimization can get stuck more easily in one of the two considered boundaries.

Table 6: Mean diameter for each district and penalization method

d_{mean} in m	Rounding	RAMP_1	RAMP_2	TH_1	TH_2	TH_3	TH_4
District 1	0.0473	0.0422	0.0465	0.0422	0.0466	0.0406	0.0423
District 2	0.0509	0.0470	0.0507	0.0470	0.0525	0.0437	0.0492
District 3	0.0458	0.0415	0.0439	0.0414	0.0453	0.0399	0.0454
District 4	0.0466	0.0422	0.0453	0.0422	0.0450	0.0398	0.0466

In Table 7, the investment costs for each district and penalization methods are shown. As the mean diameters of a district correlate with the pipe's total investment costs, the lowest costs are determined by TH_3. Due to the changing penalization direction, the investment costs determined by TH_4 are higher than by Ramp_1 and TH_1. Overall, the highest relative reduction of 6.15 % is achieved in District 2 by TH_3.

Table 7: Investment costs for each district and penalization method

C_{inv} in €	Rounding	RAMP_1	RAMP_2	TH_1	TH_2	TH_3	TH_4
District 1	477,656	459,015	474,666	458,998	475,333	453,915	459,517
District 2	677,448	656,755	669,469	656,755	679,243	635,762	668,521
District 3	939,550	914,211	929,500	914,211	936,601	902,942	936,993
District 4	1,421,084	1,373,320	1,408,253	1,373,320	1,405,552	1,351,481	1,419,541

If obtaining the lowest possible diameters is emphasized over the discretization accuracy, methods considering three diameters should be preferred over penalization methods, which only consider two diameters.

5 CONCLUSIONS

In this study, different penalization methods for discretizing continuous diameters are investigated in four real districts with an increasing number of edges and consumers. Two different penalization methods (RAMP and tangent hyperbolic) are applied on continuous diameters, obtained by a mixed integer linear programming optimization, and compared to the achieved accuracy of the final discretized diameters. In order to study the behavior of the optimization on changing penalization directions, each method is implemented once with the same penalization direction and once with changing penalization direction depending on the equation in which the penalization is used. The results of this study indicate that, based on the four considered district heating networks, all penalization methods can find a district heating configuration with a lower mean diameter and investment costs compared to rounding the continuous diameters up to the next upper commercially available diameter. Methods without changing penalization methods are shown to provide higher accuracy in the discretization of the linear pipe diameters. If the accuracy of the discretized diameter should be emphasized during the optimization, penalization methods considering two diameters should be preferred over penalization methods

https://doi.org/10.52202/077185-0022

considering three diameters. Vice-versa, if obtaining the lowest possible diameters is prioritized over the accuracy of the discretization, methods considering three diameters should be preferred. Moreover, gradient-based nonlinear optimization always converges into a local optimum; a global optimum is not guaranteed. Therefore, how different possible local minima can be compared to one another and how the optimization can efficiently choose between the various local minima that occurred during the optimization should be investigated. One possibility is the optimization with different starting values for the nonlinear phase.

REFERENCES

AGFW, 2024. *Pauschalierte Kennwerte*. https://www.fw704.de/hauptmenue/kennwerte/pauschalierte-kennwerte (accessed 22 February 2024).

Allen, A., Henze, G., Baker, K., Pavlak, G., Murphy, M., 2022. *An optimization framework for the network design of advanced district thermal energy systems.* Energy Conversion and Management 266, 115839. https://doi.org/10.1016/j.enconman.2022.115839.

Blommaert, M., Wack, Y., Baelmans, M., 2020. *An adjoint optimization approach for the topological design of large-scale district heating networks based on nonlinear models.* Applied Energy 280, 116025. https://doi.org/10.1016/j.apenergy.2020.116025.

Deaton, J.D., Grandhi, R.V., 2014. *A survey of structural and multidisciplinary continuum topology optimization: post 2000.* Structural Optimization 49, 1–38. https://doi.org/10.1007/s00158-013-0956-z.

Deng, N., Cai, R., Gao, Y., Zhou, Z., He, G., Liu, D., Zhang, A., 2017. *A MINLP model of optimal scheduling for a district heating and cooling system: A case study of an energy station in Tianjin.* Energy 141, 1750–1763. https://doi.org/10.1016/j.energy.2017.10.130.

Dorfner, J., Hamacher, T., 2014. *Large-Scale District Heating Network Optimization.* IEEE Trans. Smart Grid 5, 1884–1891. https://doi.org/10.1109/TSG.2013.2295856.

Dorfner, J., Krystallas, P., Durst, M., Massier, T., 2017. *District cooling network optimization with redundancy constraints in Singapore.* Future Cities and Environment 3, 1. https://doi.org/10.1186/s40984-016-0024-0.

European Commission, 2018. *Synthesis report on the evaluation of national notifications related to Article 14 of the Energy Efficiency Directive.* Publications Office.

Fleiter, T., Elsland, R., Rehfeldt, M., Steinbach, J., Reiter, U., Catenazzi, G., Jakob, M., Rutten, C., Harmsen, R., Dittmann, F., Rivière, P., Stabat, P., 2017. *Profile of heating and cooling demand in 2015*.

Gurobi Optimization, 2023. *Gurobi Optimization*. https://www.gurobi.com/ (accessed 22 February 2024).

Hart, W.E., Watson, J.-P., Woodruff, D.L., 2011. *Pyomo: modeling and solving mathematical programs in Python.* Math. Prog. Comp. 3, 219–260. https://doi.org/10.1007/s12532-011-0026-8.

Jodeiri, A.M., Goldsworthy, M.J., Buffa, S., Cozzini, M., 2022. *Role of sustainable heat sources in transition towards fourth generation district heating – A review.* Renewable and Sustainable Energy Reviews 158, 112156. https://doi.org/10.1016/j.rser.2022.112156.

Krogh, C., Jungersen, M.H., Lund, E., Lindgaard, E., 2017. *Gradient-based selection of cross sections: a novel approach for optimal frame structure design.* Structural Optimization 56, 959–972. https://doi.org/10.1007/s00158-017-1794-1.

Lambert, J., Ceruti, A., Spliethoff, H., 2024. *Benchmark of Milp Formulations for District Heating Network Design*.

Lambert, J., Spliethoff, H., 2023. *A Nonlinear Optimization Method for Expansion Planning of District Heating Systems with Graph Preprocessing*, in: 36th International Conference on Efficiency, Cost, Optimization, Simulation and Environmental Impact of Energy Systems (ECOS 2023): Las Palmas de Gran Canaria, Spain, 25-30 June 2023. 36th International Conference on Efficiency, Cost, Optimization, Simulation and Environmental Impact of Energy Systems (ECOS 2023), Las Palmas De Gran Canaria, Spain. 9/1/2020 - 9/5/2020. Curran Associates Inc, Red Hook, NY, pp. 2649–2660.

Lambert, J., Spliethoff, H., 2024. *Dataset for "A Two-Phase Nonlinear Optimization Method for District Heating Systems"*.

https://doi.org/10.52202/077185-0022

Merlet, Y., Baviere, R., Vasset, N., 2022. *Formulation and assessment of multi-objective optimal sizing of district heating network.* Energy 252, 123997. https://doi.org/10.1016/j.energy.2022.123997.

Mertz, T., Serra, S., Henon, A., Reneaume, J.M., 2017. *A MINLP optimization of the configuration and the design of a district heating network: study case on an existing site.* Energy Procedia 116, 236–248. https://doi.org/10.1016/j.egypro.2017.05.071.

Mertz, T., Serra, S., Henon, A., Reneaume, J.-M., 2016. *A MINLP optimization of the configuration and the design of a district heating network: Academic study cases.* Energy 117, 450–464. https://doi.org/10.1016/j.energy.2016.07.106.

Moody, L.F., 1947. *An approximate formula for pipe friction factors*.

Nussbaumer, T., Thalmann, S., 2016. *Influence of system design on heat distribution costs in district heating.* Energy 101, 496–505. https://doi.org/10.1016/j.energy.2016.02.062.

Pizzolato, A., Sciacovelli, A., Verda, V., 2018. *Topology Optimization of Robust District Heating Networks.* Journal of Energy Resources Technology 140, 020905. https://doi.org/10.1115/1.4038312.

Résimont, T., Louveaux, Q., Dewallef, P., 2021. *Optimization Tool for the Strategic Outline and Sizing of District Heating Networks Using a Geographic Information System.* Energies 14, 5575. https://doi.org/10.3390/en14175575.

Röder, J., Meyer, B., Krien, U., Zimmermann, J., Stührmann, T., Zondervan, E., 2021. *Optimal Design of District Heating Networks with Distributed Thermal Energy Storages – Method and Case Study*. 5-22 Pages / International Journal of Sustainable Energy Planning and Management, Vol. 31 (2021). https://doi.org/10.5278/ijsepm.6248.

Sigmund, O., 2001. *Design of multiphysics actuators using topology optimization – Part I: One-material structures.* Computer Methods in Applied Mechanics and Engineering 190, 6577–6604. https://doi.org/10.1016/S0045-7825(01)00251-1.

Söderman, J., 2007. *Optimisation of structure and operation of district cooling networks in urban regions.* Applied Thermal Engineering 27, 2665–2676. https://doi.org/10.1016/j.applthermaleng.2007.05.004.

Söderman, J., Pettersson, F., 2006. *Structural and operational optimisation of distributed energy systems.* Applied Thermal Engineering 26, 1400–1408. https://doi.org/10.1016/j.applthermaleng.2005.05.034.

Sporleder, M., Rath, M., Ragwitz, M., 2022. *Design optimization of district heating systems: A review.* Front. Energy Res. 10, 971912. https://doi.org/10.3389/fenrg.2022.971912.

Stanford Business Software Inc, 2021. *SNOPT*. http://www.sbsi-sol-optimize.com/asp/sol_product_snopt.htm (accessed 22 February 2024).

Umweltbundesamt, 2023. *Kohlendioxid-Emissionen im Bedarfsfeld „Wohnen“*. https://www.umweltbundesamt.de/daten/private-haushalte-konsum/wohnen/kohlendioxid-emissionen-im-bedarfsfeld-wohnen (accessed 30 January 2024).

Wack, Y., Baelmans, M., Salenbien, R., Blommaert, M., 2023a. *Economic topology optimization of District Heating Networks using a pipe penalization approach.* Energy 264, 126161. https://doi.org/10.1016/j.energy.2022.126161.

Wack, Y., Serra, S., Baelmans, M., Reneaume, J.-M., Blommaert, M., 2023b. *Nonlinear topology optimization of District Heating Networks: A benchmark of a mixed-integer and a density-based approach.* Energy 278, 127977. https://doi.org/10.1016/j.energy.2023.127977.

Werner, S., 2017. *International review of district heating and cooling.* Energy 137, 617–631. https://doi.org/10.1016/j.energy.2017.04.045.

Wu, N., Kenway, G., Mader, C., Jasa, J., Martins, J., 2020. *pyOptSparse: A Python framework for large-scale constrained nonlinear optimization of sparse systems.* JOSS 5, 2564. https://doi.org/10.21105/joss.02564.

ACKNOWLEDGEMENTS

The authors thank Benedikt Schweiger for his valuable feedback and support. This work was supported by the "Bayerische Forschungsstiftung" in the framework of the project STROM [project no.: AZ-1473-20]. The financial support is gratefully acknowledged.

https://doi.org/10.52202/077185-0022